scientific reports

Check for updates

OPEN

Chronic unpredictable stress induces anxiety-like behavior and oxidative stress, leading to diminished ovarian reserve

Zhihao Zhou[1,2,5], Yangshuo Li[1,5], Jie Ding[1,5], Shuai Sun[1], Wen Cheng[1], Jin Yu[1], Zailong Cai[3], Zhexin Ni[1,4]✉ & Chaoqin Yu[1]✉

Chronic stress can adversely affect the female reproductive endocrine system, potentially leading to disorders and impairments in ovarian function. However, current research lacks comprehensive understanding regarding the biochemical characteristics and underlying mechanisms of ovarian damage induced by chronic stress. We established a stable chronic unpredictable stress (CUS)-induced diminished ovarian reserve (DOR) animal model. Our findings demonstrated that prolonged CUS treatment over eight weeks resulted in increased atresia follicles in female mice. This atresia was accompanied by decreased AMH and increased FSH levels. Furthermore, we observed elevated levels of corticosterone both in the peripheral blood and within the ovary. Additionally, we detected abnormalities in ATP metabolism within the ovarian tissue. CUS exposure led to oxidative stress in the ovaries, fostering a microenvironment characterized by oxidative damage to mouse ovarian granulosa cells (mGCs) and heightened levels of reactive oxygen species. Furthermore, CUS prompted mGCs to undergo apoptosis via the mitochondrial pathway. These findings indicate a direct association between the fundamental physiological alterations leading to DOR and the oxidative phosphorylation processes within mGCs. The diminished ATP production by mGCs, triggered by CUS, emerges as a pivotal indicator of CUS-induced DOR. Our study establishes an animal model to investigate the impact of chronic stress on ovarian reserve function and sheds light on potential mechanisms underlying this phenomenon.

Keywords Diminished ovarian reserve, Anxiety-like behavior, Ovarian function, Chronic unpredictable stress, Oxidative stress, ATP production

Diminished ovarian reserve (DOR) implies a quantitative and qualitative decline in the oocyte pool, resulting in insufficient ovarian function and decreased fertility[1–4]. DOR is mainly divided into two types: physiological DOR related to advanced age and pathological DOR unrelated to age[2]. Recent research has revealed that the proportion of cases of pathological DOR unrelated to age is increasing, and social and psychological stress play an important role that cannot be ignored[2,5–7].

Stress is inevitable in life. Epidemiological surveys have found that[8] long-term stress will lead to a series of abnormalities in metabolism and immune system, including anxiety, depression, increased risk of cardiovascular disease, immune system disorders, endocrine disorders and reproductive dysfunction[7,8]. However, the mechanism of chronic stress leading to female reproductive endocrine system disturbance is still unclear, and many previous studies have focused on the impact of stress on the hypothalamic-pituitary-adrenal (HPA) axis. Under normal circumstances, the gonadotropin-releasing hormone (GnRH) neurons in the hypothalamus can secrete GnRH in pulses, and regulate the secretion of follicle stimulating hormone (FSH) and luteinizing hormone (LH) by the gonadotropin cells in the pituitary gland. It causes periodic secretion of estrogen and

[1]Department of Traditional Chinese Gynecology, The First Affiliated Hospital of Naval Military Medical University (Changhai Hospital), 168 Changhai Road, Yangpu District, Shanghai, China. [2]Traditional Chinese Medicine Department, No. 929 Hospital, Naval Medical University, Shanghai 200433, China. [3]Department of Biochemistry and Molecular Biology, Naval Medical University, Shanghai 200433, China. [4]Department of Pharmaceutical Sciences, Beijing Institute of Radiation Medicine, 27 Taiping Road, Haidian District, Beijing 100850, China. [5]These authors contributed equally: Zhihao Zhou, Yangshuo Li and Jie Ding. ✉email: nizxzg@163.com; chqyu81@163.com; cqyu@smmu.edu.cn

progesterone and affects reproductive system function[9]. When the body is in a state of stress, the HPA axis is activated to produce a large amount of stress hormone[10,11], which can affect the pulsatile secretion of GnRH in various ways[12–17]. However, chronic stress not only affects the hypothalamus upstream via the HPA axis, but can also directly impair ovarian function.

The mechanism through which chronic stress leads to disorders of the female reproductive endocrine system is still unclear, and the existing research has many limitations[18–20]. First and foremost is the lack of standard animal models of chronic stress-induced DOR. In addition, most of the existing animal models for stress research on are based on male mice[21]. The reason most researchers use male mice maybe that estrogen has a protective effect, but the conditions of research are obviously very different from the real world[18–20]. With the gradual development of social movements and the women's liberation movement in modern society, women's role in society and sense of empowerment is increasing daily[22,23]. However, most women experience many physiological processes, such as menstruation, leucorrhea, pregnant, birth during their lifetime, which leads to more complicated and more long-term stress than that faced by men. It has also been observed clinically that long-term exposure to various factors and compound stress can easily lead to disorders of the female reproductive endocrine system[18,22,24]. Therefore, modern research urgently needs to focus on chronic stress-induced ovarian hypofunction in women.

This study focused on the impact of chronic stress on ovarian reserve function, carried out animal modeling and effect evaluation, and revealed that chronic unpredictable stress (CUS) treatment of female mice for 8 weeks can be used to establish a DOR model. The changes in blood biochemistry and ovarian function in this model are similar to those of clinical DOR patients, and these animals can be used as a basic animal model for subsequent studies on the decline in ovarian function caused by chronic stress.

Materials and methods

Animals

Female C57 mice (15–18 g) used in our study purchased at six weeks of age from Zhejiang Vital River Experimental Animal Technology Co., Ltd [SCXK2019-0001]. The mice were kept under a temperature and humidity conditioned environment with 12 h light/dark cycle (lights on from 8:00 A.M. to 8:00 P.M.). Before experiment began, all experimental mice were allowed to adjust to the environment for at least 1 week and mice with an abnormal estrous cycle were discarded. All protocols in this animal experiment were conducted in strict accordance with the animal care and use guidelines of the Ministry of Science and Technology of the People's Republic of China, and the study was approved by Shanghai Changhai Hospital Ethics Committee [CHEC(A.E)2022-012]. All experiments were performed in accordance with relevant guidelines and regulations and the recommendations in the ARRIVE guidelines (https://arriveguidelines.org).

Stress model

The stressed groups were individually housed and received an 8-week stress procedure according to previous studies, with minor modifications[25–28]. Both the stress model group and the control group consisted of 20 mice each. The mice in the stress model group were restrained only during the daily stress procedure. Outside of these procedures, they were housed in groups of five per cage. The control group mice were also housed five per cage, with identical living conditions to the stress model group, including free access to food and water. Stress procedures included: restraint stress (1 h/d to 6 h/d), tail hanging from 10 min to 30 min, swimming in warm water (37 ℃, 15 min to 30 min), nighttime noise from 12 h to 24 h, food deprivation for 24 h, water deprivation for 24 h, reversal of the light/dark cycle for 24 h, wet pad from 12 h to 24 h, empty cage from 12 h to 24 h, Single cage feeding from 12 h to 24 h, crowded feeding from 12 h to 24 h. In CUS group, each mouse received the same daily stress stimulation, following the protocol outlined in Supplementary Tables 1–3 and Fig. 1A. Unless otherwise stated, all mice in CUS group received stress stimulation as a whole. The estrous cycle of mice in CUS group ($n=20$) and control group ($n=20$) was detected during the stress intervention and the behavioral test after the intervention was completed. For the subsequent mating experiment, other researchers randomly selected 5 animals in each group. These mated mice did not participate in other subsequent experiments. The remaining mice ($n=15$) were sacrificed for blood and ovarian tissue collection.

The description of each of the stressors used and specific stress schedule was shown in Supplementary Tables 1–3.

Estrous cycle

Our study aimed to compare the estrous phases between the CUS model and the control group during weeks 1–3 and weeks 6–8. Specifically, we assessed whether there were differences in the estrous phases between the CUS group and the control group at these two time periods. We used vaginal cytology to identify the stage of estrous cycle.

Behavioral tests

Open field test (OFT)

On day 57, following 8 weeks of stress procedures and a 24-hour rest period, OFT was conducted to evaluate the anxiety like behaviors of the mice[29]. Mice ($n=20$ per group) were placed at the periphery of an open-field area (50 cm * 50 cm) with opaque plastic walls, 40 cm in height. During the test, mice were allowed to explore the surroundings freely for 5 min. A video-tracking system (SuperMaze, Xinyuan, Shanghai) was used to measure mice's natural activity and behavior.

Elevated plus-maze test (EPM)

On day 59, EPM was conducted to evaluate the anxiety like behaviors of the mice[30]. The EPM consists of a central platform, and two closed arms (20 cm length * 12 cm height * 4 cm width) crossed with two similar

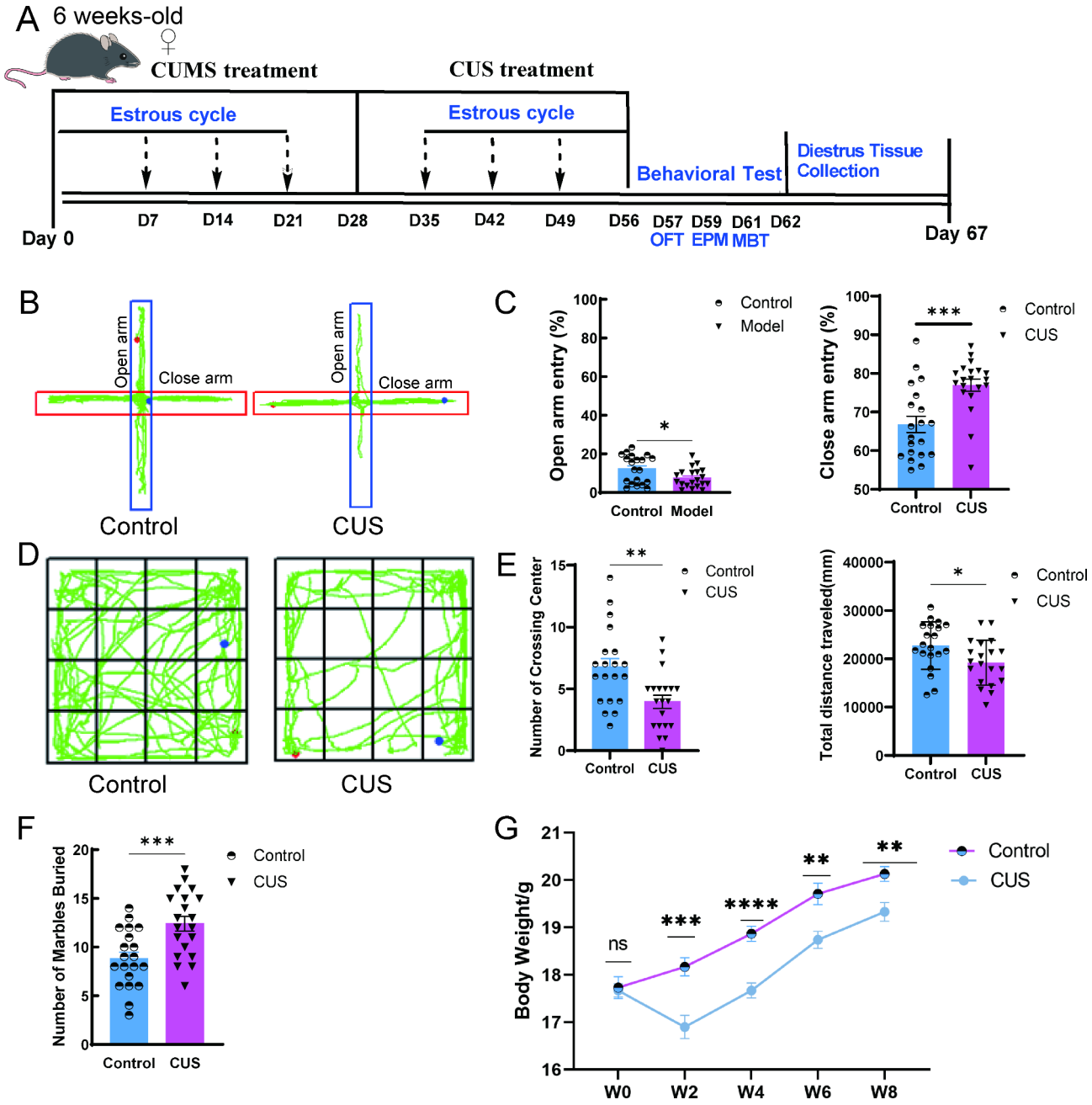

Fig. 1. CUS produces anxiety-like behavior in female mice. (**A**) Schematic representation of the experimental procedure. CUS, chronic unpredictable stress; CUMS, chronic unpredictable mild stress; OFT, Open field test; EPM, Elevated plus-maze test; MBT, Marble-burying test. (**B**) Representative exploration traces in EPM. (**C**) Percentage of time spent in the open arms and close arms of EPM ($n=20$). (**D**) Representative locomotion traces in OFT. (**E**) Number of crossing center in the central area and percentage of distance traveled in the central area of OFT ($n=20$). (**F**) Number of marbles buried in MBT ($n=20$). (G)The body weight of the CUS and control mice ($n=20$). W, week. *, $P<0.05$;**, $P<0.01$; ***, $P<0.001$.

open arms. Mice ($n=20$ per group) were placed in the central platform, and their behavior was monitored with a video-tracking system (SuperMaze, Xinyuan, Shanghai). The behavior was statistically analyzed for 5 min.

Marble-burying test (MBT)

On day 61, MBT was conducted to evaluate the anxiety like behaviors of the mice. It is based on the observation that mice have the instinct to bury dangerous objects in their living room[29]. Put 20 glass beads of the same color in a mouse cage with a size of 290 mm*180 mm*160 mm, and keep the height of the bedding not less than 100 mm. Bury it up, and evaluate the anxiety tendency of the animal by comparing the number of beads buried by the animal after 30 min. It is generally believed that the more beads' mice bury, the more anxious mice are.

Mouse tissue collection

After the completion of behavioral testing and modeling, mice were euthanized based on their estrous cycle stage, as determined by vaginal cytology. Vaginal smears were observed and recorded by an independent researcher who was blinded to the animal groups. Mice ($n=15$ per group) were euthanized during the diestrus phase to ensure consistency in the estrous cycle stage at the time of tissue collection. Serum and tissue samples were collected at 8–10 A.M. to ensure that corticosterone (CORT) levels were at baseline. This timing helps to avoid interference from daily physiological fluctuations and estrous cycle-related variations. Mice were anesthetized by intraperitoneal injection of 0.2 ml 1% Pentobarbital Sodium following Guidelines for euthanasia of experimental animals (Chinese Association for Laboratory Animal Sciences). After deep anesthesia of mice, mice blood was collected from orbit. Quickly separate ovarian tissue and place it in -80 ℃ or 4% Paraformaldehyde for further analysis.

Serum hormone assay

Serum hormone was measured by enzyme-linked immunosorbent assay (ELISA) following the manufacturer's instructions. We used commercial ELISA to access mice corticosterone (CORT, Elabsience, NO.E-OSEL-M0001), anti-mullerian hormone (AMH, Cloud-Clone Corp, NO. CEA228Mu), follicle-stimulating hormone (FSH, Cloud-Clone Corp, NO. CEA830Mu), Estradiol (E_2, Cloud-Clone Corp, NO. CEA461Ge).

Hematoxylin-eosin (HE) staining and follicle counting of ovary tissue

Pathology processing and analyses were carried out at the central laboratory of Shanghai Changhai Hospital. Briefly, one ovary was used for freezing, and the other ovary was fixed in 4% Paraformaldehyde for 24 h, and then dehydrated through a gradient of ethanol, cleared with xylene, and embedded in paraffin. To ensure accurate counting and avoid potential discrepancies caused by missing oocytes in individual sections, we performed continuous sectioning of the ovaries at 5 μm intervals and stained five consecutive sections, including the central plane of the ovary and its surrounding areas, using H&E. The data from the central plane of the ovary were used for quantification, thus minimizing the likelihood that the oocyte was missed due to it appearing in a neighboring section. Antral Follicles: Identified by the presence of an antral cavity and oocytes surrounded by more than two layers of granulosa cells. Atretic Follicles: Characterized by irregular morphology, severe nuclear displacement or condensation of the oocyte, and collapse of the zona pellucida. This methodology ensures a comprehensive assessment of follicle density and distribution across the ovary.

Mating experiments

The 10-week-old C57BL/6 N male mice were purchased from Zhejiang Vital River Laboratory Animal Technology Co., Ltd. In both the Stress and Control groups, 6 females were randomly selected for the mating experiments. For these experiments, one female from the Control group and one from the CUS group were placed together in a single cage. In each cage, we introduced a 10-week-old male with a proven reproductive history, maintaining a female-to-male ratio of 2:1. To account for individual male variability, the male mice were exchanged every 24 h over a two-week period. This approach aimed to maximize the chances of successful mating and reduce the potential influence of individual male characteristics on the reproductive outcomes. After two weeks, the male mice were removed, and the females were housed individually for 15 days to monitor pregnancy rates and subsequent reproductive outcomes.

Western blot analysis

Tissue homogenates were prepared by grinding 20 mg of ovarian tissue into ≤ 1 mm3 pieces, adding a protein lysate buffer containing RIPA (Millipore, Massachusetts, USA) with 1% PMSF (Sigma, Missouri, USA) and 1% protease inhibitor cocktail (Epizyme Biotech, GRF101, Shanghai, China). The homogenate was centrifuged for 15 min (4 °C, 12000 rpm), and the supernatant was removed. The protein concentration of the supernatant was determined using the BCA method (Sigma, Missouri, USA) and denatured by adding 5× loading buffer (Epizyme Biotech, Shanghai, China) and boiling at 99 °C for 10 min. For gel electrophoresis, the same 30ug of total protein was separated with 4 −20% sodium dodecyl sulfate – polyacrylamide gel electrophoresis (SDS-PAGE) and electro-transferred to PVDF membranes (Millipore, USA). The membranes were blocked with blocking buffer (Epizyme Biotech, PS108, Shanghai, China) for 30 min and incubated with the primary antibodies of AMH (abcam, ab229212), follicle stimulating hormone receptor (FSHR, proteintech, 22665-1-AP), BAX (proteintech, 50599-2-Ig), Bcl-2(proteintech, 68103-1-Ig), cytochrome complex (Cyt C, abcam, ab133504), beta actin (abcam, ab8226) and GAPDH (abcam, ab8245) at 4 °C for overnight. The membranes were washed with Tris Buffered Saline with Tween (TBST) thrice for 10 min each time and then incubated with HRP-conjugated secondary antibody (Epizyme Biotech, LF102; Beyotime, A0216) for 1 h at room temperature. Proteins were visualized with an ECL reagent (Millipore, Massachusetts, USA) and a champ hemi professional and automatic multicolor fluorescence and chemometric gel-imaging system (GE Healthcare ImageQuant LAS 4000mini, USA). Image J analysis software was used for densitometric analysis of immunoblots.

Transmission electron microscopy (TEM)

The ovary tissues were fixed in 2.5% glutaraldehyde fixative within 10 min after being excised. The samples were dehydrated using a density gradient of alcohol and acetone. then, the samples were cut into 60–80 nm ultrathin slices, dyed, and dried overnight at room temperature. Finally, stained with uranyl acetate and lead citrate, ovary tissues solution was observed by JEOL JEM-1230 transmission electron microscopy (80 KV).

Mitochondrial proteome sequencing

Mitochondria were extracted from primary animal samples according to the GENMED Animal Tissue Mitochondria Extraction Kit (GENMED, GMS10006.1, USA). The identification, purification and sequencing of mitochondrial proteins were assisted by Shanghai Ouyi Company (Shanghai OE Biotech. Co., Ltd.). Mechanistic research was performed with a focus on ovarian mitochondrial protein LC–MS/MS analysis. The differential proteins were screened with the absolute value of fold change greater than 1.2 and $P < 0.05$. Gene set enrichment analysis (GSEA) was performed for the differential proteins screened, False discovery rate (FDR) < 0.25, $P < 0.05$ was set as the threshold for significant results.

Ovary tissue ELISA

The ovaries ($n = 8$ per group) were first rinsed with pre-cooled PBS to remove residual blood. The tissues were then cut into small pieces, and homogenized in a tissue grinder with PBS at a 1:9 weight-to-volume ratio. The homogenate was subjected to ice-cold grinding and then centrifuged at 3000 rpm for 10 min. The supernatant was collected for analysis. Oxidative stress evaluation was mainly relying on ELISA and spectrophotometric assay kits. We used commercial ELISA to access mice ovary tissue reactive oxygen species (ROS, SunLong Biotech Co.,LTD, SL0771Mo), malondialdehyde (MDA, Elabsience, E-EL-0060c), superoxide dismutase (SOD, Cloud-Clone Corp, NO. SES134Mu. Adenosine 5'-triphosphate (ATP, Beyotime, S0026) and total antioxidant capacity (T-AOC, Beyotime, S0121) were measured by spectrophotometric assay kits.

Isolation and culture of mGCs

Mice were intraperitoneally injected with pregnant horse serum gonadotropin (10 IU, Ningbo Sanseng Pharmaceutical Co., Ltd, Zhejiang, China). After 48 h, the mice were sacrificed under 1% pentobarbital sodium anesthesia, and then bilateral ovaries were removed. Mince the ovaries on the sterile operating table, Add IV collagenase at a volume ratio of 1:5, digest in a water bath at 37 °C for 0.5 h, and shake the reaction system every 5 min. Next, we filtered the mixture through a 70 μm cell strainer (BD Falcon, USA), and then centrifuged at 1200 g for 5 min. The supernatant was discarded, and the granulosa cells were obtained. The cells (1×10^5 cells/T25) were continuously cultured in Dulbecco's modified Eagle medium (DMEM) containing 10% fetal bovine serum (FBS) at 37 °C and 5% CO_2.

Immunofluorescence staining identification of mGCs

The above mice ovarian granulosa cell was fixed with 4% paraformaldehyde for 15 to 20 min at room temperature and permeabilized with 0.1% Triton X-100 for 10 min at room temperature. Cells were then blocked with blocking solution for 30 min and incubated with primary antibodies FSHR polyclonal antibody (Proteintech, 22665-1-AP, rabbit anti mouse, 1:200) overnight at 4 °C. Nucleus was stained with DAPI (Beyotime, C1005). Images were obtained and analyzed using Olympus FV1000 confocal microscope (Olympus, FV1000, Japan).

Primary mGCs apoptosis detection

An Annexin V-FITC/PI apoptosis detection kit (BD Pharmingen™, 556547, USA) was used to visualize apoptotic cells according to the manufacturer's instructions. A total of 1×10^6 primary mGCs were collected, washed with ice-cold PBS twice and resuspended in 300 μL of Annexin V binding buffer. Next, 5 μL of Annexin V-FITC was added to the cell suspension and incubated at room temperature for 15 min. Next, 200 μL of Annexin V binding buffer was added, and the samples were analyzed with a flow cytometer with PI added to the cell suspension.

Primary mGCs ROS and JC-1

A reactive oxygen species assay kit (Beyotime, S0033S) was used to visualize primary mGCs ROS according to the manufacturer's instructions. Briefly speaking, A total of 1×10^6 primary mGCs were cultured in the 24-well plates at a density of 2.5×10^5cells/mL in DMEM medium containing 10% FBS.

After 24 h, the cells were gently washed with PBS followed by the incubation with 10 μmol/L DCFH-DA at 37 °C for 18 min. The dye was then removed and replaced with fresh PBS 3 times. Images were obtained by Olympus microscope.

A mitochondrion staining kit (JC-1) (Multi Sciences, MJ101) was used to visualize detection of mitochondrial membrane potential according to the manufacturer's instructions. A total of 1×10^6 primary mGCs were collected, washed with warm staining buffer twice and resuspended in 1 μL of JC-1 (make sure jc-1 final concentration 2 μmol/L and incubated at room temperature for 30 min). Resuspend the cells used 500 μL of warm PBS. Next the samples were analyzed with a flow cytometer with 488 nm.

Seahorse XF cell mitochondrial/glycolysis stress test assay

The primary mGCs from each group were extracted for the Seahorse Glycolysis Stress Test and Seahorse Cell Mito Stress Test to verify the mitochondrial proteomic results. The Seahorse XF experiments were conducted using the Agilent Seahorse Extracellular Flux (XF) Pro analyzer. The following kits were used: Seahorse XF Cell Mitochondrial Stress Test Assay and Seahorse XF Cell Glycolysis Stress Test Assay.

Cell line

The human ovarian granulosa-like tumor cell line KGN was obtained from EK Bioscience (Shanghai, China). Primary mouse ovarian granulosa cells(mGCs) were extracted from CUS group mice and Control group mice. Cells were cultured in Dulbecco's modified Eagle's medium (DMEM, Gibco, New York, USA) with 10% fetal bovine serum (FBS, Gibco, New York, USA) and penicillin-streptomycin (10000 U/mL, Gibco, New York, USA), and then maintained at 37 °C with 5% CO2. Hydrogen peroxide solution (Sigma Aldrich, H1009) was purchased from Sigma Biotechnology. The solutions were then diluted with DMEM to achieve the desired concentrations

of H2O2 (0–1 μmol/L -10 μmol/L -30 μmol/L -100 μmol/L -300 μmol/L -1000 μmol/L − 3000 μmol/L) for the KGN standard curve. H2O2 at 200 μmol/L was used to induce oxidative stress. Dexamethasone (DEX) solution (MCE, State of New Jersey, USA) was dissolved in DMSO and prepared with blank DMEM. The final system DMSO was less than 1/1000, containing 10% FBS, 100 U/mL penicillin and 100 μg/mL streptomycin, and the final concentration of DEX was 0.25 μmol/L. Vitamin E (Sangon Biotech, A506770-0025) was dissolved in DMSO. The final system DMSO was less than 1/1000, containing 10% FBS and 100 U/mL penicillin and 100 μg/mL streptomycin. The final concentration of Vitamin E was 200 μmol/L. KGN Cells were treated with or without 200 μmol/L H2O2 or treated with 0.25 μmol/L DEX + H2O2 solution or 200 μmol/L Vitamin E + H2O2 solution for 24 h. Cell viability was analyzed using Cell Counting Kit 8 assay (CCK8, absin. abs50003).

Intracellular colocalization of Mito-Tracker Green and Lyso-Tracker red test

The Mitochondrion were detected using Mito-Tracker Green (Thermo Fisher Scientific Inc. M46750). After being cultured on sterile culture dishes, each group of treated KGN cells were incubated with 20 nM Mito-Tracker Green at 37 °C for 22 min. The cells were then washed with PBS to remove any excess Mito marker and visualized using an Olympus microscope (System Microscope BX53, Japan). The cells were then washed with PBS again. Each group of treated KGN cells were incubated with 50 nM Lyso-Tracker Red (Beyotime C1046, Shanghai, China) at 37 °C for 20 min. The cells were then washed with PBS to remove any excess lysosomal marker and visualized using an Olympus microscope (System Microscope BX53, Japan). Using Hoechst (20 mM) (Thermo Fisher Scientific Inc. 62249) to detected cell nucleus.

Statistical analyses

All statistical analysis was done using GraphPad version 9.0 software. The results were shown as means ± standard error (means ± SEM). The Student's t-test was used for comparison between the two groups, differences were defined as statistically significant with a $P < 0.05$ at a 95% confidence level.

Results

CUS produces anxiety-like behavior in female mice

The chronic unpredictable stimulation procedure can be found in Supplement Tables 1, 2 and 3 and consisted mainly of restraint, tail-spinning, fatigue swimming, nighttime noise, horizontal oscillation, diurnal reversal, wet bedding, empty cage, strobe, single cage feeding, crowded feeding, fasting and water deprivation, with two stressors randomly applied daily during the day and night. The modelling procedure and treatments for the CUS model in mice are shown in Fig. 1A and detailed details can be found in Materials and Methods 2.2. After 8 weeks of unpredictable stimulation, the CUS group exhibited a lower proportion of open-arm time and a higher proportion of closed-arm time in the EPM compared to the control group (Fig. 1B and C). In the OFT, the CUS group showed significantly lower autonomous exploratory behavior (Fig. 1D and E). As well as in the MBT, the number of buried beads was significantly higher in the CUS group (Fig. 1F). In addition, the body weight of mice in the CUS group was significantly lower than the control group (Fig. 1G). In conclusion, the three behavioral experiments showed that mice exhibited anxiety-like behavioral changes after CUS.

CUS induce stress in female mice and impair reproductive function

It is not known whether female mice develop DOR following the development of anxiety-like behavioral changes. So, we further investigated the impairment of ovarian function in mice with CUS. First, the estrous cycle of the CUS group was disturbed (Fig. 2A), as evidenced by a shortened estrus phase and an extended prolonged diestrus in the mice. Subsequently, we further examined the serum sex hormone levels in the mice, in which the AMH levels were significantly lower and the FSH levels were significantly higher in the CUS group compared to the control group (Fig. 2B, $P < 0.05$). and E_2 levels increased, the difference was not statistically significant ($P > 0.05$). As AMH is a key indicator to characterize DOR, we further illustrated by Western-blot that AMH expression was significantly reduced in ovarian tissues of the CUS group (Fig. 2E). In addition, FSHR, which is expressed on the surface of ovarian granulosa cells and binds to FSH to activate a complex signaling network that promotes follicle growth and maturation, was reduced in the CUS group (Fig. 2E). Follicle development in the CUS group was with a significant decrease in the number of antral follicles and a significant increase in the number of atretic follicles (Fig. 2C). Finally, the results of the mating experiments showed that the three-week litter survival rate was reduced in the CUS group (Fig. 2D). In conclusion, our results suggest that CUS treatment of female mice for 8 weeks can stably produce anxiety-like behavior that led to DOR.

Mitochondrial proteome sequencing reveals the effect pathway of CUS treatment on the ovary

Cortisol plays an important role in coping with stress and is known as the "stress hormone"[10,11,31]. We found significantly higher serum and ovarian cortisol levels in the CUS group of mice (Fig. 3A and B). Previous literature has shown that chronic stress is associated with impaired mitochondrial function[32–34] and that local enrichment of cortisol leads to altered mitochondrial membrane shape[35,36]. Correspondingly, we observed CUS leads to abnormal mitochondrial morphology such as smaller body size, smaller cristae and denser matrix by TEM (Fig. 3C). Therefore, we further investigated the pathway of CUS action on mitochondrial damage in ovarian granulosa cells. Mitochondrial proteome sequencing results showed that 39 proteins were significantly differentially expressed between the CUS and control group, of which 29 were up-regulated and 10 were down-regulated (|Fold change|>1.2, $P < 0.05$, Fig. 3D and E). Further GSEA revealed 4 potential pathways of action mediating the mitochondrial damage of CUS on ovarian granulosa cells, including redox homeostasis, glycolytic gluconeogenesis, oxidative phosphorylation and apoptosis (Fig. 3F-I). These results suggest that CUS may promote DOR formation by inducing alterations in mitochondrial function in ovarian granulosa cells.

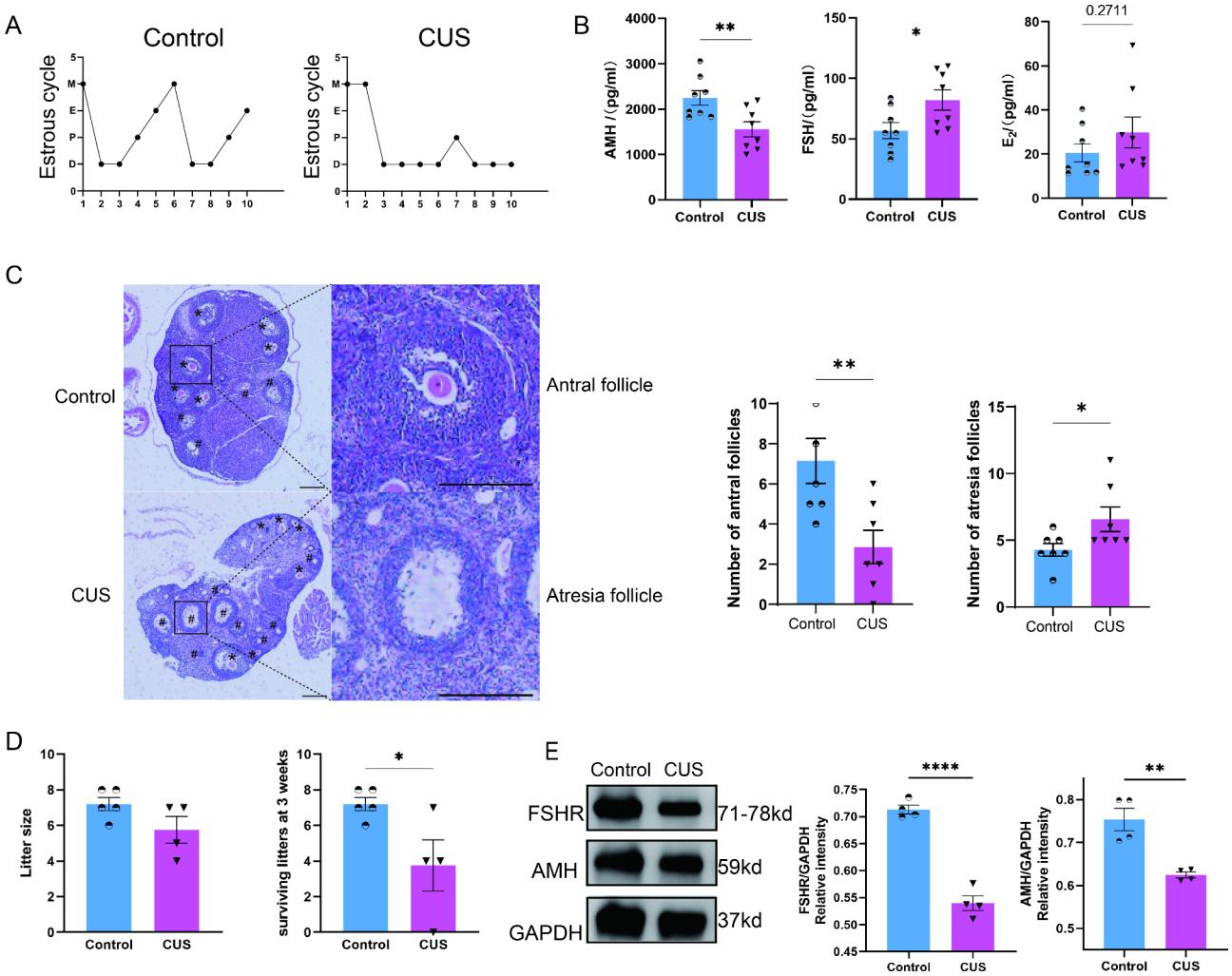

Fig. 2. CUS induce stress in female mice and impair reproductive function. (**A**) Representative images exhibiting the changes of female mice estrous cycle for 10 consecutive days. P, proestrus; E, estrus; M, metestrus; D, diestrus. (**B**) Serum reproductive hormone concentrations ($n=8$). AMH, anti-mullerian hormone; FSH, follicle stimulating hormone; E_2, estradiol. (**C**) Representative HE staining images of mice ovarian tissues from CUS and control group ($n=7$). (**D**) The number of pups born (left) and the number of pups surviving (right) at three weeks were recorded for each pregnant female ($n=5$ in Control; $n=4$ in CUS). (**E**) Protein expression analysis of AMH and FSHR in the ovaries ($n=4$). FSHR, follicle stimulating hormone receptor. *, $P<0.05$; **, $P<0.01$; ****, $P<0.0001$.

CUS promotes ovarian granulosa cell oxidative stress and mitochondrial membrane potential change and triggers apoptosis

Based on the above mitochondrial proteome sequencing results, we focused on three aspects: oxidative stress, apoptosis and energy metabolism. Firstly, we measured ROS, MDA and ATP levels in the ovaries, where ROS and MDA levels were significantly higher and ATP levels were significantly lower in the CUS group compared to the control group (Fig. 4A), indicating that oxidative damage occurred in the CUS group. To investigate whether damage to the antioxidant system occurred, we further explored SOD and T-AOC. SOD and T-AOC levels were significantly lower in the CUS group compared to the control group (Fig. 4B). These results suggest that CUS causes oxidative stress in the ovaries and may impair antioxidant capacity. Subsequently, we extracted primary mGCs from mice for subsequent studies. The immunofluorescence results showed increased levels of ROS in the CUS group (Fig. 4C), consistent with previous studies.

Subsequently, we continued to explore the apoptotic pathway. Flow cytometric analysis showed an increased rate of apoptosis in the mGCs of the CUS group (Fig. 4E), and the formation of apoptotic vesicles could be observed under TEM (Fig. 4D). To further investigate the pathways causing apoptosis, we examined the expression levels of the apoptosis-related proteins BAX and BCL-2 in the ovaries of each group of mice (Fig. 4F), which showed that BAX expression was increased and BCL-2 expression was reduced in the CUS group.

An early and distinctive feature of the early stages of apoptosis is damage to active mitochondria, including alterations in membrane potential as well as alterations in mitochondrial oxidation-reduction potential[37]. The reason for the altered membrane potential may be due to the opening of the mitochondrial transition pore,

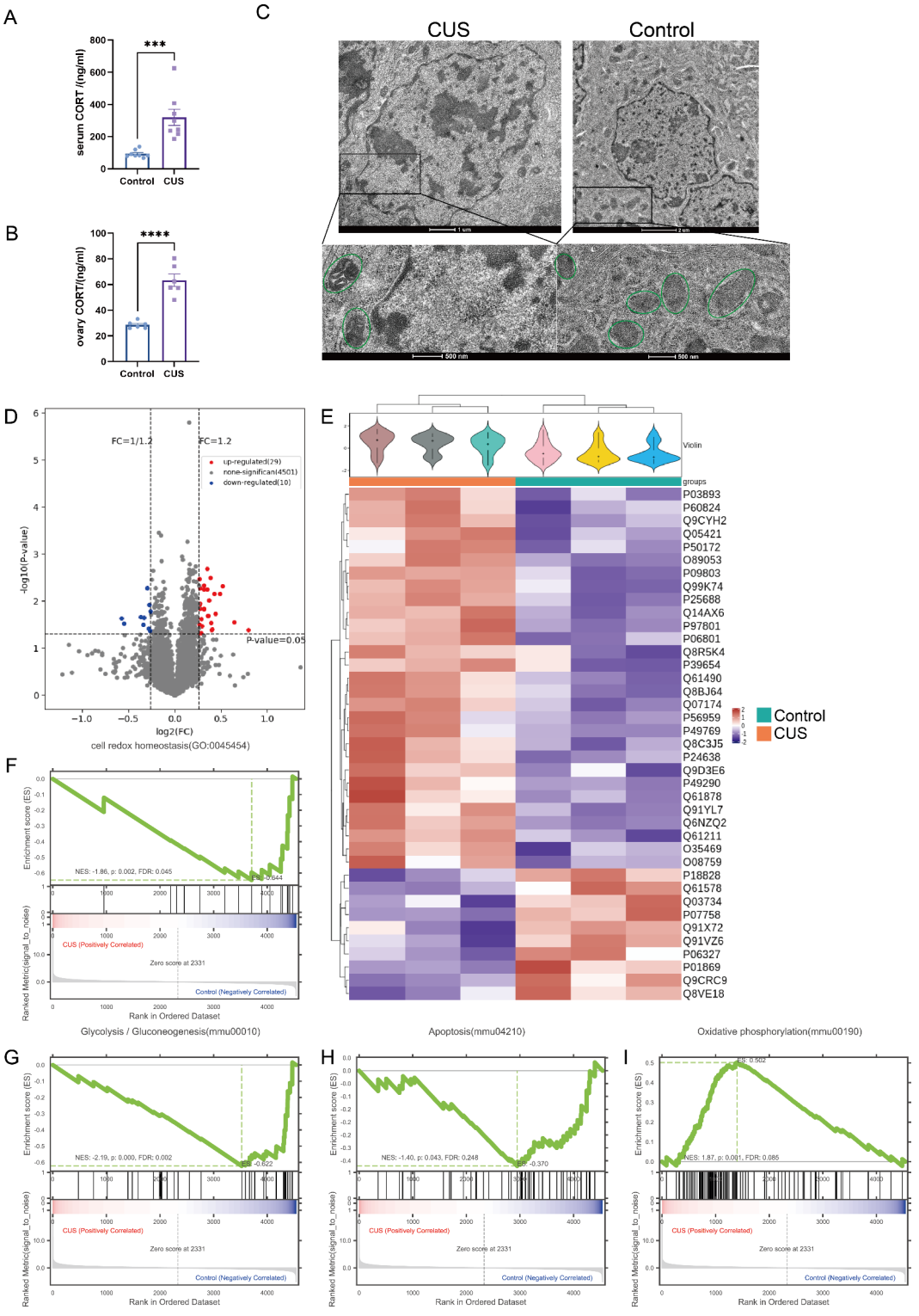

Fig. 3. Mitochondrial proteome sequencing support CUS induce alterations in mitochondrial function in mGCs. (**A** and **B**) CUS produces CORT rising in female mice blood and ovary ($n=8$). CORT, corticosterone. (**C**) CUS leads to abnormal mitochondrial morphology by TEM. (**D**) Volcano plot of mitochondrial proteins with log2 ratio of abundance of CUS/Control (x axis) and the –log10 of the corresponding significance value (P value, y axis); 1.2-fold changes (vertical lines), significance cutoff $P=0.05$ (horizontal line). (**E**) Unsupervised heatmap cluster analysis of all detected mitochondrial proteins. CUS, red; control, blue. ($n=3$) (**F**–**I**) Examples of 4 terms identified by GSEA. (**F**) Cell redox homeostasis (GO:0045454), FDR = 0.045 $P=0.002$. (**G**) Glycolysis / Gluconeogenesis(mmu00010), FDR = 0.045 $P<0.001$. (**H**) Apoptosis(mmu04210), FDR = 0.248, $P=0.043$. (**I**) Oxidative phosphorylation (mmu00190), FDR = 0.085 $P=0.001$.

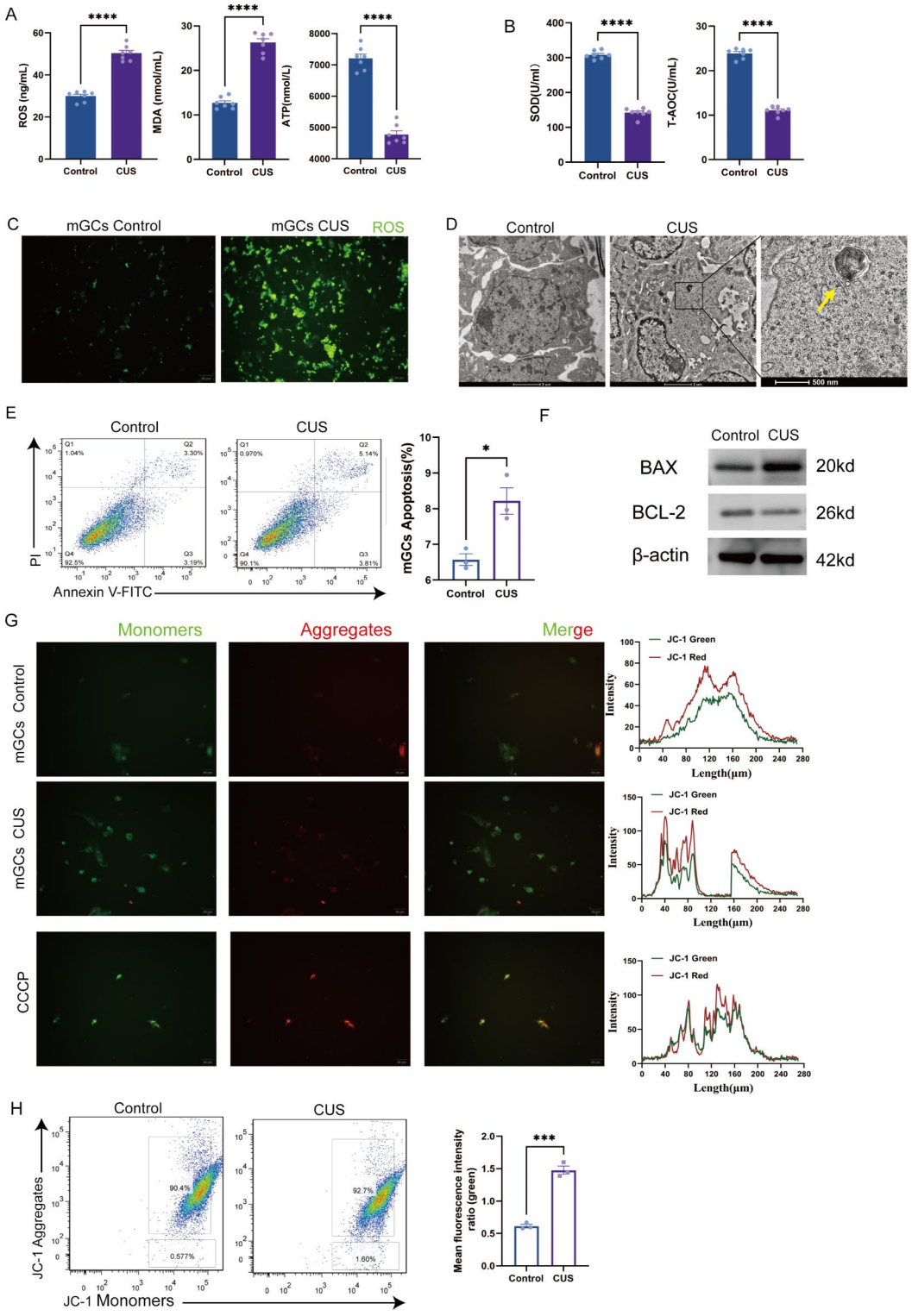

Fig. 4. CUS promotes mGCs oxidative stress and mitochondrial membrane potential change and triggers apoptosis. (**A**) Level of ROS, MDA, ATP measured by ELISA in ovary tissues ($n=7$). (**B**) SOD, T-AOC measured by ELISA in ovary tissues ($n=7$). (**C**) ROS fluorescence detection between mGCs from CUS group and Control group. (**D**) mGCs from CUS group find apoptosis body by TEM. (**E**) Detection of apoptosis in mGCs by flow cytometry ($n=3$). (**F**) Protein expression analysis of BAX and BCL-2 in the ovaries. (**G**) JC-1 specifically detected mitochondrial membrane potential excitation at 405 nm fluorescence detection. (**H**) Mitochondrial membrane potential specifically detected with JC-1 in mGCs by flow cytometry ($n=3$). *, $P<0.05$; **, $P<0.01$; ***, $P<0.001$; ****, $P<0.0001$.

leading to the entry of ions and small molecules into the mitochondria[38]. The resulting ion homeostasis decouples the respiratory chain, which in turn releases Cytochrome C into the cytoplasm. Cytochrome C can activate the downstream caspase family and induce apoptosis. In combination with previous literature, we hypothesized that apoptosis may occur as a result of damage to the mitochondrial membrane. Therefore, we further explored the alteration of mitochondrial membrane potential by CUS. Our JC-1 fluorescence results showed elevated numbers of JC-1 monomers in granulosa cells in the CUS group (Fig. 4G, JC-1 green light), indicating a decrease in mitochondrial membrane potential. Subsequent flow analysis also showed the same result (Fig. 4H). Taken together, these data suggest that CUS may lead to altered mitochondrial membrane potential in mGCs and may further induce oxidative stress and apoptosis.

Effect of CUS on glycolysis level and mitochondrial function in mGCs

In this section we explored the energy metabolism-related pathways of CUS causing DOR, and the Seahorse results revealed that CUS had essentially no effect on the level of glycolysis in mGCs (Fig. 5A-D). Interestingly, after performing O_2 consumption rate (OCR), an experiment to quantify mitochondrial functional parameters, we found significant differences in basal respiration, maximal respiration and ATP production in mGCs in the CUS group compared to the control group (Fig. 5E-H). These results suggest that mGCs abnormal oxidative phosphorylation may also be part of the evidence that CUS causes DOR.

Granulosa cells under simulated oxidative stress microenvironment in vitro

Based on the above in vivo studies in mice and the primary mGCs cell results, we further used the human ovarian granulosa cell line KGN to provide evidence. In vitro intervention of KGN by hydrogen peroxide (H_2O_2) induced cellular oxidative stress[39,40] mimicking local oxidative damage in the ovary due to chronic stress. In addition, organisms under chronic stress conditions are hyper-functional in the hypothalamic-pituitary-adrenal axis and glucocorticoid secretion is elevated in the body to adapt to the environment[41]. In order to investigate the effect of glucocorticoids themselves on the granulosa cells of the ovary, we added exogenous dexamethasone (DEX), and since vitamin E (Vit E), an essential vitamin, plays an important antioxidant role[42], we further investigated whether Vit E could play a mitigating role in oxidative stress.

After determining the optimal concentrations of H_2O_2, DEX and Vit E intervention, we divided the experimental control group, the H_2O_2 group, the H_2O_2 + DEX group and the H_2O_2 + Vit E group into the following groups. Immunofluorescence assays showed that ROS levels were elevated in the H_2O_2 group compared to the control group, while the Vit E intervention partially alleviated the elevated ROS (Fig. 6A). In addition, the apoptotic ratio of KGN cells in different groups was further detected by flow cytometry. It was found that DEX and Vit E could effectively improve the apoptotic effect of H_2O_2, and the effect of Vit E was more obvious (Fig. 6B). These data suggest that Vit E can partially reduce the proportion of apoptosis caused by H_2O_2 and protect KGN cells. Subsequently, we examined the KGN mitochondrial membrane potential using the same method as before and showed that the proportion of depolarized mitochondrial membrane potential was higher in the H_2O_2 group and the H_2O_2 + DEX group (Fig. 6C), while the mitochondrial membrane potential depolarization was significantly lower in the Vit E + H_2O_2-intervened KGN cells than in the H_2O_2 group. On the other hand, a lysosomal fluorescent probe was invoked to further probe the effect of oxidative stress on outer mitochondrial membrane function. The fluorescence probe results showed more co-localization between the mitochondrial and lysosomal probes induced in the H_2O_2 group and the H_2O_2 + DEX group (Fig. 6D). The reduced fluorescence intensity of the lysosomal probe in the Vit E + H_2O_2 interfered KGN cells suggested that Vit E protection of the mitochondrial membrane potential might be associated with stabilization of the lysosome.

Discussion

Studies have pointed out that stress can reduce the production of estradiol by affecting the function of granulosa cells in follicles, thereby leading to the deterioration of oocyte quality[43].

Our study focuses on the effects of chronic stress on ovarian function. Psychological stress was induced in mice treated with CUS for 8 weeks. As a classical model of depression, CUS induced typical anxiety-like behaviors in OFT, EPM as well as MBT, indicators that mice are experiencing psychological stress.

The core feature of the clinical diagnosis of DOR is the impairment of ovarian function or the presence of decreased oocyte quality[44]. There are no accepted diagnostic criteria for DOR, and a comprehensive assessment of ovarian reserve function is currently based on indicators such as AMH, FSH, E_2 and AFC. We verified this by looking at the rate of estrous cycle disturbance, peripheral blood AMH, FSH and E_2 levels, number of antral follicle and atretic follicles, mating experiment, ovarian AMH and FSHR, and other indicators from multiple perspectives. In conclusion, these results suggest that CUS-treated female mice diminished ovarian reserve and induced DOR phenotype. The human reproductive cycle is characterized by single-follicle developmental ovulation and selective ovulation. In the ovary, the granulosa cell surface of the developing follicle specifically expresses FSHR[45], which binds specifically to FSH secreted by the hypothalamus, activating a complex signaling network that promotes follicle growth and maturation[45–47]. These signaling pathways downstream promote granulosa cell proliferation, and induce aromatase expression and estrogen synthesis[46,48]. In addition, AMH is secreted by small immature ovarian follicular granulosa cells. AMH levels in the blood are stable, do not fluctuate with the menstrual cycle or with the presence or absence of pregnancy, and can indicate the stock power of ovarian follicles, which is an important predictor of fertility[49]. Our results show that the low expression of FSHR and AMH protein levels in mouse ovaries after CUS affects follicular development. These results further suggest that chronic stress can directly lead to a decrease in ovarian reserve function.

Mice which were administered CORT for 21 days showed typical depressive behavior[36,50,51]. Our results show that both peripheral blood and ovarian CORT levels are significantly increased in mice after CUS. Increased CORT levels can lead to the development of oxidative stress and anxiety behaviors[36], while excess CORT in the

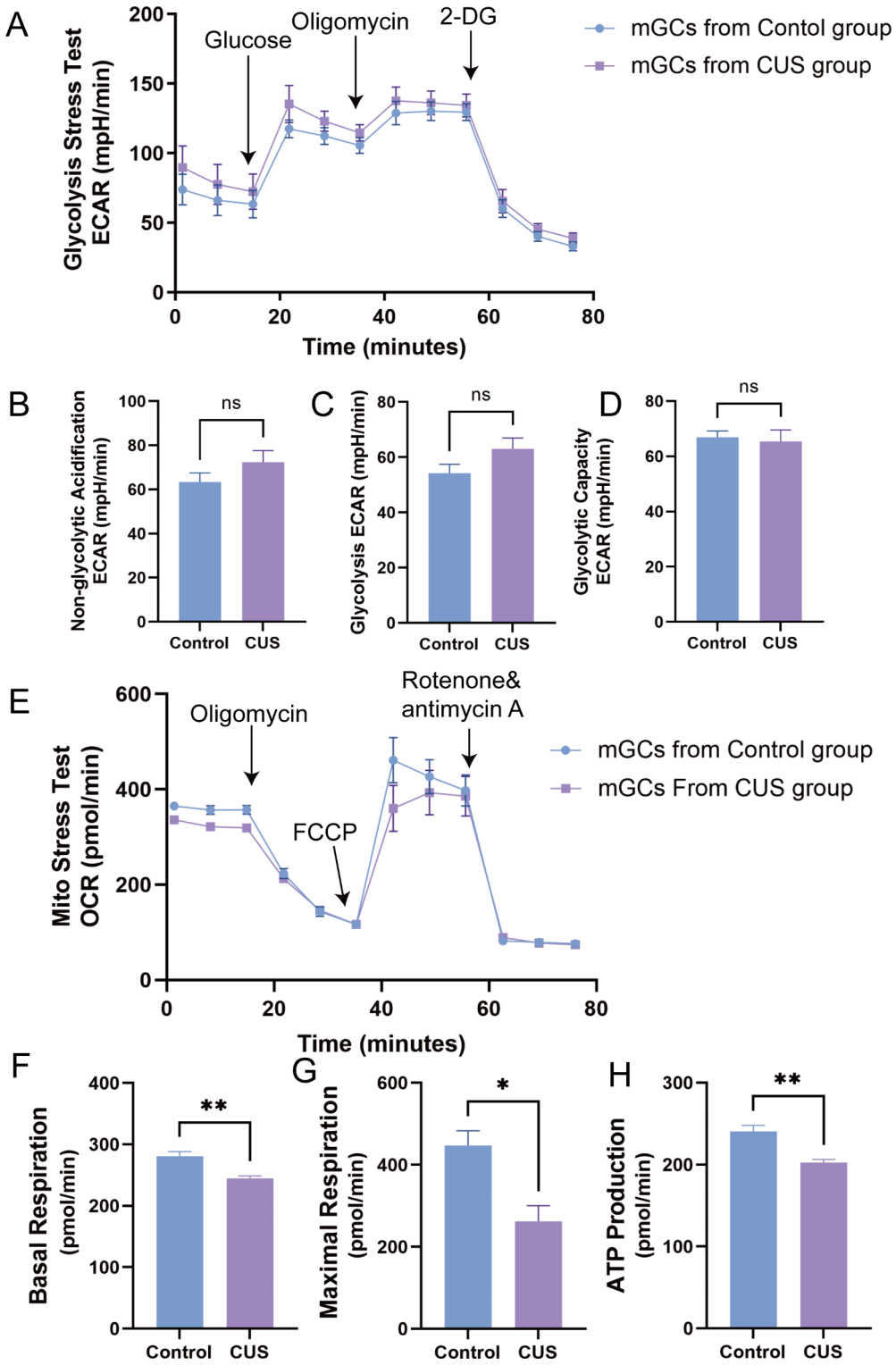

Fig. 5. Effect of CUS on glycolysis level and mitochondrial function in mGCs. (**A**) The mGCs analyze extracellular acidification rate (ECAR) by Seahorse Glycolytic Rate Assay (Glucose:10mM Glucose, Oligomycin: electron transport chain(ETC) complex IV inhibitors, 2-DG: 2-deoxy-glucose, hexokinase competitive inhibitors). (**B**–**D**) Non-glycolytic acidification, glycolysis and glycolytic capacity in seahorse glycolytic stress test assay; (**E**) The mGCs analyze oxygen consumption rate (OCR) by seahorse Mito stress assay (FCCP: Carbonyl cyanide-4 (trifluoromethoxy)Phenylhydrazone, Mitochondrial uncouplers that completely disrupt proton gradients and mitochondrial membrane potential, Rotenone: ETC complex I inhibitors, Antimycin A: ETC complex III inhibitors). (**F**–**H**) Basal respiration, maximal respiration and ATP production in seahorse Mito stress assay. ns, no significance; *, $P < 0.05$; **, $P < 0.01$.

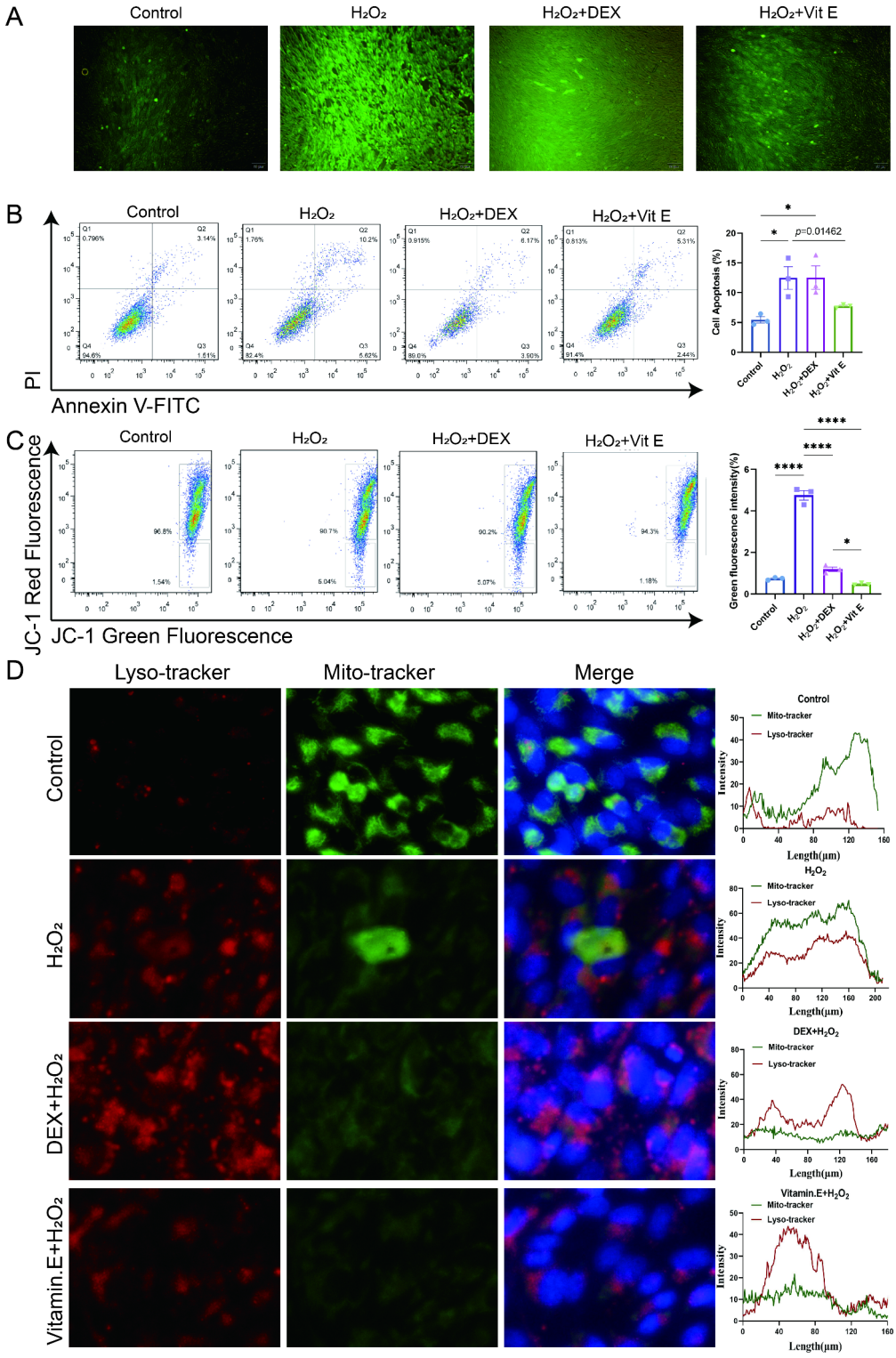

Fig. 6. Effect of oxidative stress on granulosa cell function in vitro. (**A**) ROS fluorescence detection between KGN cell among control group, H_2O_2 group, H_2O_2 + DEX group and H_2O_2 + Vitamin E group. DEX, dexamethasone; Vit E, vitamin E. (**B**) Detection of apoptosis in KGN by flow cytometry. (**C**) Mitochondrial membrane potential specifically detected with JC-1 in KGN by flow cytometry. (**D**) The relative expression level of Lysotracker and Mito tracker in KGN. *, $P < 0.05$; **, $P < 0.01$; ***, $P < 0.001$; ****, $P < 0.0001$.

ovary contributes to the production and accumulation of ROS[43,52], which is the source of the active substance causing oxidative damage[53]. Thus, excess CORT forms an ovarian oxidative stress microenvironment that further impairs female oocyte development and granulosa cell proliferation[32,52,54]. In addition, the oxidative stress microenvironment itself can lead to apoptosis in ovarian granulosa cells[52,55], with the early stages of apoptosis notably characterized by impaired mitochondrial activity, including alterations in membrane potential and oxidation-reduction potential[37]. Chronic stress may affect mitochondrial membrane permeability, leading to increased proton leakage and increased ROS production, both of which can affect the stability of mitochondrial DNA as well as mitochondrial function[32,34]. Our results show that CUS can induce apoptosis in ovarian granulosa cells with apoptotic vesicles. Further detection of mitochondrial depolarization by binding of JC-1 to granulosa cells showed that the membrane potential of granulosa cells from mice undergoing CUS was altered, possibly due to the opening of the mitochondrial transition pore, which drives ions and small molecules into the mitochondria[38]. The resulting disruption of ionic homeostasis decouples the respiratory chain, leading to the entry of substances such as cytochrome complex into the cytoplasm of the mitochondria, activating the downstream caspase family. The pro-apoptotic protein BAX and the anti-apoptotic protein BCL-2 further demonstrate that CUS induces apoptosis in granulosa cells via the mitochondrial pathway.

Whole-exome sequencing of mitochondrial DNA from ovarian granulosa cells of patients with DOR has shown that mutations in the cytochrome oxidase 1 gene of mitochondrial DNA led to a reduction in the number of mitochondria and impaired energy metabolism[56]. However, the Seahorse glycolytic stress test revealed no direct correlation between CUS-induced physiological alterations in DOR and the glycolytic process in mouse ovarian granules. In contrast, we found differences in parameters such as nonmitochondrial respiration, basal respiration, maximal respiration, and ATP production by the Seahorse mitochondrial function test. This suggests that CUS can cause abnormal oxidative phosphorylation in granulosa cells, leading to reduced ATP production, which may be another potential etiology for DOR formation.

By introducing KGN as the research object and using H_2O_2 to induce oxidative stress in KGN, we have determined that the oxidative damage microenvironment with high ROS can induce ovarian granulosa cell apoptosis, and exogenous DEX cannot alleviate cell apoptosis and mitochondrial depolarization, Vit .E can improve oxidative stress and resist apoptosis; the protection of ovarian granulosa cells by Vit E may be related to the stability of lysosomes, and its specific molecular mechanism is worthy of further exploration.

In this study, animal models were made and their effects were evaluated in order to investigate the effects of chronic stress on ovarian reserve function and its possible mechanisms. A DOR model was found to be induced in female mice treated with CUS for 8 weeks. The blood biochemical and ovarian function changes in this model were similar to those in clinical DOR patients, which can be used as a basic animal model for subsequent studies on the decline of ovarian function due to chronic stress. Unfortunately, we lack clinical samples to enrich our research. Through mitochondrial proteomic sequencing and cross-validation of in vivo and in vitro experiments, we found that CUS-induced DOR mice had elevated levels of stress CORT in peripheral blood and ovaries, which could induce local oxidative stress in ovaries and form a high ROS oxidative damage microenvironment. Such microenvironment induced an increased rate of apoptosis and mitochondrial depolarization in mouse ovarian granulosa cells. In addition, CUS-associated abnormalities in ovarian energy metabolism in DOR mice were directly associated with abnormal oxidative phosphorylation of ovarian granulosa cells. The final in vitro investigation provides a possible therapeutic approach for ovarian granulosa cell oxidative stress.

Data availability

The datasets used and/or analyzed during the current study are available from the corresponding author on reasonable request.

Received: 3 July 2024; Accepted: 16 October 2024
Published online: 28 December 2024

References

1. Testing Interpreting measures of ovarian reserve: a committee opinion. *Fertil. Steril.* **114**, 1151–1157. https://doi.org/10.1016/j.fertnstert.2020.09.134 (2020).
2. Pastore, L. M., Christianson, M. S., Stelling, J., Kearns, W. G. & Segars, J. H. Reproductive ovarian testing and the alphabet soup of diagnoses: DOR, POI, POF, POR, and FOR. *J. Assist. Reprod. Genet.* **35**, 17–23. https://doi.org/10.1007/s10815-017-1058-4 (2018).
3. Tal, R. & Seifer, D. B. Ovarian reserve testing: a user's guide. *Am. J. Obstet. Gynecol.* **217**, 129–140. https://doi.org/10.1016/j.ajog.2017.02.027 (2017).
4. Cedars, M. I. Evaluation of female fertility-AMH and ovarian reserve testing. *J. Clin. Endocrinol. Metab.* **107**, 1510–1519. https://doi.org/10.1210/clinem/dgac039 (2022).
5. Schliep, K. C. et al. Perceived stress, reproductive hormones, and ovulatory function: a prospective cohort study. *Epidemiology*. **26**, 177–184. https://doi.org/10.1097/ede.0000000000000238 (2015).
6. Zhang, Q. L. et al. Treatment progress in diminished ovarian reserve: western and Chinese medicine. *Chin. J. Integr. Med.* https://doi.org/10.1007/s11655-021-3353-2 (2022).
7. Pal, L., Bevilacqua, K. & Santoro, N. F. Chronic psychosocial stressors are detrimental to ovarian reserve: a study of infertile women. *J. Psychosom. Obstet. Gynaecol.* **31**, 130–139. https://doi.org/10.3109/0167482x.2010.485258 (2010).
8. Cohen, S., Gianaros, P. J. & Manuck, S. B. A stage model of stress and disease. *Perspect. Psychol. Sci.* **11**, 456–463. https://doi.org/10.1177/1745691616646305 (2016).
9. Herbison, A. E. The gonadotropin-releasing hormone pulse generator. *Endocrinology*. **159**, 3723–3736. https://doi.org/10.1210/en.2018-00653 (2018).
10. Galluzzi, L., Yamazaki, T. & Kroemer, G. Linking cellular stress responses to systemic homeostasis. *Nat. Rev. Mol. Cell. Biol.* **19**, 731–745. https://doi.org/10.1038/s41580-018-0068-0 (2018).
11. Russell, G. & Lightman, S. The human stress response. *Nat. Rev. Endocrinol.* **15**, 525–534. https://doi.org/10.1038/s41574-019-0228-0 (2019).

12. Moore, A. M., Coolen, L. M., Porter, D. T., Goodman, R. L. & Lehman, M. N. *KNDy Cells Revisit. Endocrinol.* **159**, 3219–3234, doi:https://doi.org/10.1210/en.2018-00389 (2018).
13. Merkley, C. M., Coolen, L. M., Goodman, R. L. & Lehman, M. N. Evidence for changes in numbers of synaptic inputs onto KNDy and GnRH neurones during the preovulatory LH surge in the ewe. *J. Neuroendocrinol.* **27**, 624–635. https://doi.org/10.1111/jne.12293 (2015).
14. Sánchez-Garrido, M. A., García-Galiano, D. & Tena-Sempere, M. Early programming of reproductive health and fertility: novel neuroendocrine mechanisms and implications in reproductive medicine. *Hum. Reprod. Update*. **28**, 346–375. https://doi.org/10.1093/humupd/dmac005 (2022).
15. Yang, J. A. et al. Acute psychosocial stress inhibits LH pulsatility and Kiss1 neuronal activation in female mice. *Endocrinology*. **158**, 3716–3723. https://doi.org/10.1210/en.2017-00301 (2017).
16. Kim, J. S. et al. Anxiogenic and stressor effects of the hypothalamic neuropeptide RFRP-3 are overcome by the NPFFR antagonist GJ14. *Endocrinology*. **156**, 4152–4162. https://doi.org/10.1210/en.2015-1532 (2015).
17. Geraghty, A. C. et al. Knockdown of hypothalamic RFRP3 prevents chronic stress-induced infertility and embryo resorption. *Elife*. **4**https://doi.org/10.7554/eLife.04316 (2015).
18. Heck, A. L. & Handa, R. J. Sex differences in the hypothalamic-pituitary-adrenal axis' response to stress: an important role for gonadal hormones. *Neuropsychopharmacology*. **44**, 45–58. https://doi.org/10.1038/s41386-018-0167-9 (2019).
19. Labonté, B. et al. Sex-specific transcriptional signatures in human depression. *Nat. Med.* **23**, 1102–1111. https://doi.org/10.1038/nm.4386 (2017).
20. Zefferino, R., Di Gioia, S. & Conese, M. Molecular links between endocrine, nervous and immune system during chronic stress. *Brain Behav.* **11**, e01960. https://doi.org/10.1002/brb3.1960 (2021).
21. Tan, T. et al. Neural circuits and activity dynamics underlying sex-specific effects of chronic social isolation stress. *Cell. Rep.* **34**, 108874. https://doi.org/10.1016/j.celrep.2021.108874 (2021).
22. Handa, R. J. & Weiser, M. J. Gonadal steroid hormones and the hypothalamo-pituitary-adrenal axis. *Front. Neuroendocrinol.* **35**, 197–220. https://doi.org/10.1016/j.yfrne.2013.11.001 (2014).
23. Do, D. & Schnittker, J. Pharmaceutical side effects and the sex differences in depression and distress. *Am. J. Prev. Med.* **63**, 213–224. https://doi.org/10.1016/j.amepre.2022.01.036 (2022).
24. Wirth, M. M. Beyond the HPA Axis: progesterone-derived neuroactive steroids in human stress and emotion. *Front. Endocrinol. (Lausanne)*. **2**https://doi.org/10.3389/fendo.2011.00019 (2011).
25. Gao, L., Zhao, F., Zhang, Y., Wang, W. & Cao, Q. Diminished ovarian reserve induced by chronic unpredictable stress in C57BL/6 mice. *Gynecol. Endocrinol.* **36**, 49–54. https://doi.org/10.1080/09513590.2019.1631274 (2020).
26. Katz, R. J. Animal model of depression: pharmacological sensitivity of a hedonic deficit. *Pharmacol. Biochem. Behav.* **16**, 965–968. https://doi.org/10.1016/0091-3057(82)90053-3 (1982).
27. Qiao, H. et al. Dendritic spines in depression: what we learned from animal models. *Neural Plast.* **2016** (8056370). https://doi.org/10.1155/2016/8056370 (2016).
28. Picard, K. et al. Microglial-glucocorticoid receptor depletion alters the response of hippocampal microglia and neurons in a chronic unpredictable mild stress paradigm in female mice. *Brain Behav. Immun.* **97**, 423–439. https://doi.org/10.1016/j.bbi.2021.07.022 (2021).
29. Sturman, O., Germain, P. L. & Bohacek, J. Exploratory rearing: a context- and stress-sensitive behavior recorded in the open-field test. *Stress*. **21**, 443–452. https://doi.org/10.1080/10253890.2018.1438405 (2018).
30. Rodgers, R. J. & Dalvi, A. Anxiety, defence and the elevated plus-maze. *Neurosci. Biobehav Rev.* **21**, 801–810. https://doi.org/10.1016/s0149-7634(96)00058-9 (1997).
31. Kim, Y. K., Na, K. S., Myint, A. M. & Leonard, B. E. The role of pro-inflammatory cytokines in neuroinflammation, neurogenesis and the neuroendocrine system in major depression. *Prog Neuropsychopharmacol. Biol. Psychiatry*. **64**, 277–284. https://doi.org/10.1016/j.pnpbp.2015.06.008 (2016).
32. Filomeni, G., De Zio, D. & Cecconi, F. Oxidative stress and autophagy: the clash between damage and metabolic needs. *Cell. Death Differ.* **22**, 377–388. https://doi.org/10.1038/cdd.2014.150 (2015).
33. Zhang, T. et al. Mitochondrial dysfunction and endoplasmic reticulum stress involved in oocyte aging: an analysis using single-cell RNA-sequencing of mouse oocytes. *J. Ovarian Res.* **12**, 53. https://doi.org/10.1186/s13048-019-0529-x (2019).
34. Sahin, E. & DePinho, R. A. Axis of ageing: telomeres, p53 and mitochondria. *Nat. Rev. Mol. Cell. Biol.* **13**, 397–404. https://doi.org/10.1038/nrm3352 (2012).
35. Choi, G. E. et al. BNIP3L/NIX-mediated mitophagy protects against glucocorticoid-induced synapse defects. *Nat. Commun.* **12**, 487. https://doi.org/10.1038/s41467-020-20679-y (2021).
36. Camargo, A. et al. Cholecalciferol counteracts depressive-like behavior and oxidative stress induced by repeated corticosterone treatment in mice. *Eur. J. Pharmacol.* **833**, 451–461. https://doi.org/10.1016/j.ejphar.2018.07.002 (2018).
37. Ma, X. et al. Prussian blue nanozyme as a pyroptosis inhibitor alleviates neurodegeneration. *Adv. Mater.* **34**, e2106723. https://doi.org/10.1002/adma.202106723 (2022).
38. Han, X. et al. Neuronal SH2B1 attenuates apoptosis in an MPTP mouse model of Parkinson's disease via promoting PLIN4 degradation. *Redox Biol.* **52**, 102308. https://doi.org/10.1016/j.redox.2022.102308 (2022).
39. Xin, X., Gong, T. & Hong, Y. Hydrogen peroxide initiates oxidative stress and proteomic alterations in meningothelial cells. *Sci. Rep.* **12**, 14519. https://doi.org/10.1038/s41598-022-18548-3 (2022).
40. Sies, H. Oxidative eustress: on constant alert for redox homeostasis. *Redox Biol.* **41**, 101867. https://doi.org/10.1016/j.redox.2021.101867 (2021).
41. Prasad, S., Tiwari, M., Pandey, A. N., Shrivastav, T. G. & Chaube, S. K. Impact of stress on oocyte quality and reproductive outcome. *J. Biomed. Sci.* **23**, 36. https://doi.org/10.1186/s12929-016-0253-4 (2016).
42. Miyazawa, T. et al. Regulatory redox interactions. *IUBMB Life*. **71**, 430–441. https://doi.org/10.1002/iub.2008 (2019).
43. Ebbesen, S. M. et al. Stressful life events are associated with a poor in-vitro fertilization (IVF) outcome: a prospective study. *Hum. Reprod.* **24**, 2173–2182. https://doi.org/10.1093/humrep/dep185 (2009).
44. Busnelli, A., Somigliana, E., Cirillo, F. & Levi-Setti, P. E. Is diminished ovarian reserve a risk factor for miscarriage? Results of a systematic review and meta-analysis. *Hum. Reprod. Update*. **27**, 973–988. https://doi.org/10.1093/humupd/dmab018 (2021).
45. Bhartiya, D. & Patel, H. An overview of FSH-FSHR biology and explaining the existing conundrums. *J. Ovarian Res.* **14**https://doi.org/10.1186/s13048-021-00880-3 (2021).
46. Recchia, K. et al. Actions and roles of FSH in germinative cells. *Int. J. Mol. Sci.* **22**https://doi.org/10.3390/ijms221810110 (2021).
47. Stamatiades, G. A., Carroll, R. S. & Kaiser, U. B. GnRH-A key regulator of FSH. *Endocrinology*. **160**, 57–67. https://doi.org/10.1210/en.2018-00889 (2019).
48. Agwuegbo, U. T. et al. Differential FSH glycosylation modulates FSHR oligomerization and subsequent cAMP signaling. *Front. Endocrinol. (Lausanne)*. **12**, 765727. https://doi.org/10.3389/fendo.2021.765727 (2021).
49. Santoro, N. Using antimüllerian hormone to predict fertility. *Jama*. **318**, 1333–1334. https://doi.org/10.1001/jama.2017.14954 (2017).
50. Camargo, A., Dalmagro, A. P., de Souza, M. M., Zeni, A. L. B. & Rodrigues, A. L. S. Ketamine, but not guanosine, as a prophylactic agent against corticosterone-induced depressive-like behavior: possible role of long-lasting pro-synaptogenic signaling pathway. *Exp. Neurol.* **334**, 113459. https://doi.org/10.1016/j.expneurol.2020.113459 (2020).

51. Camargo, A. et al. A low-dose combination of ketamine and guanosine counteracts corticosterone-induced depressive-like behavior and hippocampal synaptic impairments via mTORC1 signaling. *Prog Neuropsychopharmacol. Biol. Psychiatry*. **111**, 110371. https://doi.org/10.1016/j.pnpbp.2021.110371 (2021).
52. Wang, L. et al. Oxidative stress in oocyte aging and female reproduction. *J. Cell. Physiol.* **236**, 7966–7983. https://doi.org/10.1002/jcp.30468 (2021).
53. Zhang, B. et al. Role of mitochondrial reactive oxygen species in homeostasis regulation. *Redox Rep.* **27**, 45–52. https://doi.org/10.1080/13510002.2022.2046423 (2022).
54. Kala, M. & Nivsarkar, M. Role of cortisol and superoxide dismutase in psychological stress induced anovulation. *Gen. Comp. Endocrinol.* **225**, 117–124. https://doi.org/10.1016/j.ygcen.2015.09.010 (2016).
55. Sinha, K., Das, J., Pal, P. B. & Sil, P. C. Oxidative stress: the mitochondria-dependent and mitochondria-independent pathways of apoptosis. *Arch. Toxicol.* **87**, 1157–1180. https://doi.org/10.1007/s00204-013-1034-4 (2013).
56. Zhen, X. et al. Increased incidence of mitochondrial cytochrome C oxidase 1 gene mutations in patients with primary ovarian insufficiency. *PLoS One*. **10**, e0132610. https://doi.org/10.1371/journal.pone.0132610 (2015).

Acknowledgements

This work was supported by the "Dark Blue 123" Military Medicine Special - Free Exploration Project [2020SLZ020], the Science and Technology Innovation Action Plan of Shanghai Science and Technology Commission [20Z21900405], the Natural Science Foundation of China [82074206], the Natural Science Foundation of Shanghai [23ZR1478600] and the Shanghai Traditional Chinese Medicine Academic Experience Research Studio of Eminent Practitioners [SHGZS-202240].

Author contributions

Z.Z, Y.L., and J.D. contributed equally to this work. C.Y., Z.N., Z.C. and Z.Z. designed the experiments and analyzed the data. Z.Z. and Y.L. wrote the manuscript. J.D. and Z.Z. performed the majority of the experiments. S.S, W.C., and J.Y. assisted with the animal experiments. Z.Z. and Y.L. contributed to the study design and manuscript preparation.All authors reviewed the manuscript.

Declarations

Competing interests

The authors declare no competing interests.

Accordance

All experiments were performed in accordance with relevant guidelines and regulations and the recommendations in the ARRIVE guidelines.

Additional information

Supplementary Information The online version contains supplementary material available at https://doi.org/10.1038/s41598-024-76717-y.

Correspondence and requests for materials should be addressed to Z.N. or C.Y.